

## A COMPLETE CO SURVEY OF M31

E. KOPER,<sup>1</sup> T. M. DAME,<sup>2</sup> F. P. ISRAEL,<sup>1</sup> AND P. THADDEUS<sup>2</sup>

Received 1991 July 3; accepted 1991 September 18

### ABSTRACT

M31 was fully surveyed at an angular resolution of 8'7 in the  $J = 1 \rightarrow 0$  rotational transition of CO. The  $153' \times 45'$  area observed covers the entire galaxy to a radius of at least 16 kpc, well beyond the optical disk and Population I peak at 10 kpc. The bulk of the CO emission lies between 8 and 11 kpc from the galactic center. Compared with H I, the CO emission is more confined to optical Population I and tends to peak  $\sim 1$  kpc closer to the center. Although previously few CO observations have been directed toward the NE tangent of the Population I ring, it appears as rich in molecular gas as the SW tangent. Little CO emission is found within 8 kpc of the center of M31. Using the Galactic value for the conversion of integrated CO intensity to  $H_2$  mass, the total molecular mass of M31 is  $\sim 2.5 \times 10^8 M_\odot$ , less than one-fourth the molecular mass of the Milky Way computed in the same way.

*Subject headings:* galaxies: interstellar matter — galaxies: Local Group — interstellar: matter — interstellar: molecules

To study the distribution of molecular gas in the disk of M31 we undertook a complete CO survey. Although the global distributions of two other major constituents of the interstellar medium, H I (e.g., Cram, Roberts, & Whitehurst 1980; hereafter CRW) and warm dust (Walterbos & Schwering 1987), have been well determined, only a modest fraction of its disk (less than 10% of the area covered by our survey) had previously been observed in CO (e.g., Stark, Linke, & Frerking 1981; Ryden & Stark 1986)—and very much less than that in any other molecule. The difficulty is mainly the large angular size of M31, especially compared with the beam sizes of millimeter telescopes, as well as the weakness of CO in the galaxy.

Our CO survey of M31 was conducted during two 6 month periods in the colder months of 1989–1991, with on average 8 hours observation per day with the 1.2 m telescope at the Center for Astrophysics. This instrument is well-matched to the task: its 65 K single-sideband SIS receiver is one of the most sensitive now operating at 115 GHz, and its 8'7 beam is small enough to allow good determination of the radial distribution of CO in M31 but large enough to allow a fully sampled survey in 1 or 2 years. The spectrometer used for the survey, a filter bank of 256 channels each 0.5 MHz wide, provided more than adequate velocity resolution ( $1.3 \text{ km s}^{-1}$ ) and coverage ( $332 \text{ km s}^{-1}$ ) for the broad CO lines observed in a spiral galaxy viewed only  $13^\circ$  from edge on.

Because the beam of the 1.2 m telescope at 115 GHz is almost exactly equal to that of the Bonn 100 m telescope at 21 cm, we observed on the same Baade-Arp ( $X, Y$ ) grid as the 21 cm survey of CRW. The 365 positions observed, spaced every half-beamwidth (4'5) within an area of  $153' \times 45'$ , completely cover M31 out to a radius  $R$  of 16 kpc—well beyond the peak in Population I at 10 kpc. Between  $R = 16$  and 21 kpc about 70% of the area was covered. Each position was observed at least 5 times on different days for a total integration time per position of  $\sim 100$  minutes and  $\sigma(T_R) < 18 \text{ mK}$ —more sensitive than that of any previous extended CO survey in any object.

Even with such high sensitivity, typical CO lines have peak

temperatures only a few times the single-channel noise, but the lines are so wide—of order 75 channels ( $\sim 100 \text{ km s}^{-1}$ )—that integrated intensities are fairly well determined if baseline curvature can be eliminated as a source of systematic error. Consistently flat baselines were achieved by fast position switching in azimuth with a period of only 20 s to the nearest point beyond the H I disk observed by CRW. To keep residual (ON-OFF) powers low and suppress baseline irregularities caused by small nonlinearities of the backend filters, the ON-OFF difference in elevation was adjusted after each position-switching cycle to cancel fluctuations in atmospheric emission (mainly from clouds) and changes in receiver gain. By moving the OFF just a few arcminutes above or below the ON in elevation, total system temperatures at the two positions could generally be held equal to better than 1 part in  $10^4$ . A small fraction of the observations ( $< 5\%$ ) for which the residual power was greater than 0.1 K were repeated.

The CO spectrum averaged over the entire Population I ring of M31 (i.e., all spectra in the range  $R = 6\text{--}12$  kpc) is shown in Figure 1, with the tenfold more intense spectrum at the peak CO position in the insert, and, for comparison, the corresponding 21 cm lines scaled down by a factor of  $10^3$ . The average CO and H I profiles are quite similar in shape, both showing the double-peaked profile characteristic of an inclined rotating disk. The close similarity of the profiles near the extreme velocities ( $-550$  and  $-50 \text{ km s}^{-1}$ ), despite differences in the radial distributions of CO and H I (discussed below), indicates that both species follow the same flat rotation curve in the range  $R = 6\text{--}12$  kpc.

The best overall summary of our survey, a map of velocity-integrated CO intensity,  $W_{\text{CO}}$ , smoothed slightly to  $10'$  to enhance the signal-to-noise ratio, is compared in Figure 2 to similarly smoothed maps of H I column density and IRAS 100  $\mu\text{m}$  emission. Integration over the wide CO lines of M31 yields a signal-to-noise ratio in  $W_{\text{CO}}$  at least a factor of 5 higher than that in individual unsmoothed spectra. Over most of the molecular disk, the main uncertainty in determining the total ( $H_2$ ) molecular column density is probably not in the statistical or systematic uncertainties in our data but in the standard assumption that  $W_{\text{CO}}$  is a reliable tracer of molecular mass.

The most conspicuous feature common to all three maps is

<sup>1</sup> Leiden Observatory, P.O. Box 9513, 2300 RA Leiden, The Netherlands.

<sup>2</sup> Harvard-Smithsonian Center for Astrophysics, 60 Garden Street, Cambridge, MA 02138.

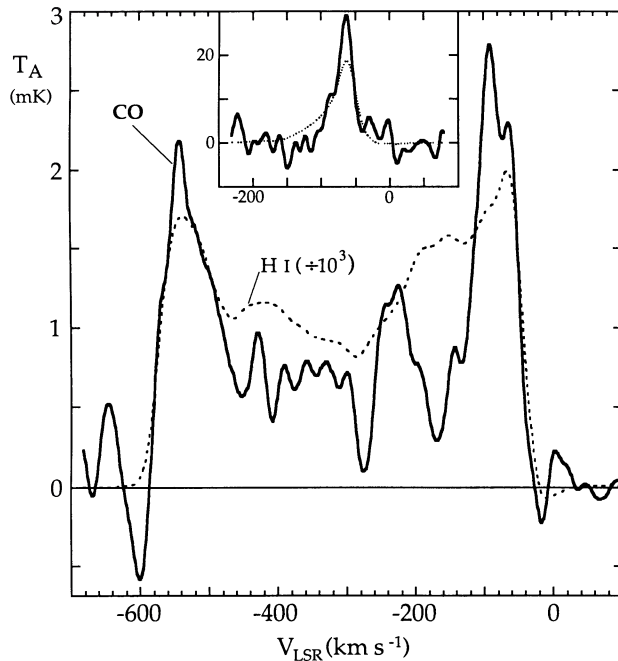


FIG. 1.—CO emission from the Population I ring of M31, an average of all spectra between galactic radii 6 and 12 kpc, compared with the thousandfold more intense H I 21 cm line. The CO profile has been smoothed to a velocity resolution of  $20 \text{ km s}^{-1}$ . In the same units, the insert shows CO and H I at the peak CO position (the average of the four spectra within a half-beamwidth of  $[X, Y] = 47.25, 2.25$ ), both smoothed to a velocity resolution of  $10 \text{ km s}^{-1}$ .

the enhancement of emission at  $\sim 10 \text{ kpc}$  from the center ( $\sim 50'$  along the major axis). We will refer to this feature as a ring, by analogy with our own galaxy, even though in M31 as here the ring is almost certainly resolvable into spiral arms and is hence quite nonaxisymmetric. The smoother appearance of the H I compared with CO may be partially attributed to the larger H I scale height, coupled with the high inclination of the disk (Boulanger, Stark, & Combes 1981), but it is also likely that, as in the Milky Way, the molecular gas is intrinsically more clumped than H I. The radial extent of the CO appears similar to that of the  $100 \mu\text{m}$  emission, and considerably less than that of H I; the secondary maxima in the  $N_{\text{HI}}$  map at roughly  $70'$  in either direction from the center along the major axis, corresponding to the optical spiral arms N5 and S5 identified by Arp (1964), are far less pronounced in the  $W_{\text{CO}}$  and  $100 \mu\text{m}$  maps.

In marked contrast to the Milky Way and most other Sb and Sc spirals observed to date (Young & Scoville 1991), the central region of M31 is quite deficient in both atomic and molecular gas but intense at  $100 \mu\text{m}$ . This infrared emission is probably from dust in fairly low-density gas heated by red giants in the nuclear bulge (Habing et al. 1984). Owing to the limited angular resolution of our survey the reality of the vertical bridge of emission just right of the center in Figure 2b at  $X = 9'$  might be questioned, but the 6 cm continuum survey of Berkhuijsen, Wielebinski, & Beck (1983) shows a general enhancement of emission in this region and two strong sources (5C 3.111 and 5C 3.119) both within  $1'$  of SNRs identified by D'Odorico, Dopita, & Benvenuti (1980, their nos. 13 and 15, respectively). Another CO peak inside the main ring, near  $(X, Y) = (-18', 0')$ , is nearly coincident with two prominent dark clouds near the tip of Arp's (1964) spiral arm S3.

A prominent gap in the ring appears in the upper left of all

three maps, near  $(-27', 9')$ , a region where Berkhuijsen, Beck, & Gräve (1987) find a large-scale disturbance of the magnetic field, and Walterbos & Schwering (1987) find a large  $20'$  far-infrared spur (below the lowest contour in Fig. 2c), suggesting ejection of material. Another gap in the CO ring appears at a nearly symmetric position on the opposite side of the galactic center, near  $(27', -9')$ . It is apparent also at  $100 \mu\text{m}$  and in maps of other Population I such as radio continuum (Berkhuijsen et al. 1983; Berkhuijsen 1977) and H II regions (Pellet et al. 1978) but not in  $N_{\text{HI}}$ .

Most of the previous partial CO mapping of M31 has been within our highest few contours in the region of intense emission near the SW tangent of the ring (e.g., Stark et al. 1981; Boulanger et al. 1981; Boulanger et al. 1984; Ichikawa et al. 1985; Lada et al. 1988; Boulanger et al. 1988), a peak at  $100 \mu\text{m}$  coinciding with one of the most conspicuous optical dust lanes. Since the high CO intensity of this region is at least partly attributable to the long line of sight through the ring at its tangent, the  $\sim 5'$  displacement of the peak intensity from the major axis, apparent in all three maps in Figure 2, is significant, an indication of warping of the galactic plane. Arp (1964) and others have found evidence of a similar displacement of the main spiral arm in this direction.

The next largest region of M31 previously studied in CO (Ryden & Stark 1986) is a  $4' \times 20'$  area roughly following the ridge of strong  $100 \mu\text{m}$  emission well above the major axis in the eastern quadrant ( $22.5', 9'$ ). Although we find fairly strong CO emission there, even stronger is found just off the SW edge of Ryden & Stark's map (at  $X < 18'$ ) in a region slightly weaker at  $100 \mu\text{m}$  and 21 cm but with comparable emission at 6 cm (Berkhuijsen et al. 1983) and a comparable number density of H II regions (Berkhuijsen 1977).

The SW and NE tangent regions of M31 are compared quantitatively in Figure 3a, which shows  $W_{\text{CO}}$  and  $N_{\text{HI}}$  averaged over a strip  $9'$  wide centered on the major axis. The figure clearly shows that the main CO peaks lie  $\sim 5'$ , or 1 kpc, inward of the H I peaks. Such offsets are evident on both sides of the galaxy, even though on the NE side the peaks, both H I and CO, are shifted outward by  $\sim 5'$  relative to the SW peaks. Since higher resolution studies near the major axis have not found any systematic offset between H I and CO spiral arms (e.g., Stark 1985), it is likely that the offset observed here merely reflects the lower mean radius of molecular gas compared with H I.

Almost no previous CO observations were directed toward the NE tangent of the ring ( $45', 0'$ ), but, as Figures 2 and 3a show, the CO emission there is as extended at our resolution as at the well-studied SW tangent, and more intense by  $\sim 20\%$ . The NE tangent may have been neglected because an early study of CO along the major axis by Combes et al. (1977) suggested that the SW side was the richer in molecular gas, and because of the absence of a strong far-infrared peak or large dust lanes as conspicuous in optical photos as those near the SW tangent—though Hodge (1980) finds that the number of dust lanes are comparable in the vicinity of the two tangent points.

The high angle of inclination of M31 precludes direct determination of the molecular distribution along its minor axis with our data, given our projected resolution along this axis of about 7 kpc. To determine the distribution with  $R$  of the molecular gas using all our spectra, we fitted an inclined axisymmetric disk to the velocity-integrated CO emission using the iterative procedure of Lucy (1974). The CO surface

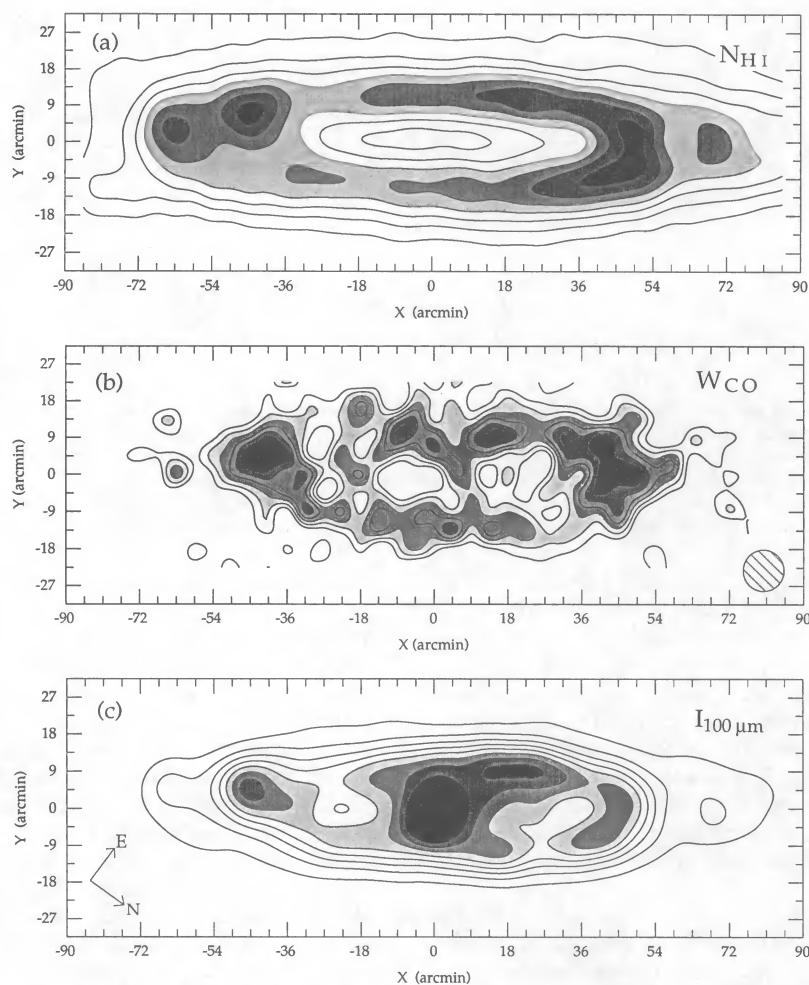


FIG. 2.—Comparison of gas tracers in M31.  $X$  and  $Y$  are Baade-Arp offsets from  $\alpha = 0^{\text{h}}40^{\text{m}}$ ,  $\delta = 41^{\circ}$  along and perpendicular to the major axis, at p.a.  $38^{\circ}$ . The maps are spatially smoothed to an angular resolution of  $10'$ . (a) H I column density derived from the 21 cm survey of CRW with foreground emission from the Milky Way removed; the contour interval is  $2.4 \times 10^{20} \text{ cm}^{-2}$ . (b) Velocity-integrated CO intensity; the contour interval is  $0.18 \text{ K km s}^{-1}$ , about the  $1 \sigma$  noise level. The hatched beam represents the  $10'$  angular resolution of all three maps. (c) IRAS  $100 \mu\text{m}$  emission; the contour interval is  $1.8 \text{ MJy sr}^{-1}$ .

brightness was converted to  $\text{H}_2$  face-on mass surface density on the assumption that  $X \equiv N(\text{H}_2)/W_{\text{CO}} = 2.3 \times 10^{20} \text{ cm}^{-2} \text{ K}^{-1} \text{ km}^{-1} \text{ s}$ , the conversion ratio determined from an inter-comparison of gas tracers and  $\gamma$ -rays in the Milky Way (Strong et al. 1988). For comparison, and as a check on the procedure, a similar axisymmetric model was fitted to the velocity-integrated 21 cm data of CRW; the results of both fits are shown in Figure 3b. The H I radial distribution agrees quite well with that derived from a simple radial binning of interferometric 21 cm data obtained by Unwin (1980) at a resolution of about  $1'$ .

Both the H I and  $\text{H}_2$  densities rise smoothly to a peak near 10 kpc, although, as already evident along the major axis (Fig. 3a), the  $\text{H}_2$  is displaced inward by  $\sim 1$  kpc relative to the H I. The most conspicuous difference between the density profiles is the much sharper drop in  $\text{H}_2$  beyond 10 kpc—an effect which is almost certainly real because of the similar ways in which the H I and CO data were taken, the similar angular resolutions, and the identical method of data analysis. Near the peak of the M31 molecular ring we derive an average molecular surface density of  $\sim 1 M_{\odot} \text{ pc}^{-2}$ , about 3 times less than the atomic

surface density there and about 6 times less than the molecular surface density at the peak of the Milky Way molecular ring (Bronfman et al. 1988, scaled slightly to the  $X$ -ratio adopted here). Integration over radius yields a total  $\text{H}_2$  mass for M31 of  $2.5 \pm 0.2 \times 10^8 M_{\odot}$ , about 4 times less than the  $\text{H}_2$  mass of the Milky Way computed in the same way:  $11 \times 10^8 M_{\odot}$  (Bronfman et al. 1988, Digel 1991; all results scaled to the  $X$ -ratio adopted here and to  $R_{\odot} = 8.5$  kpc) and more than an order of magnitude less than the total atomic mass of M31 determined by CRW:  $3.9 \times 10^9 M_{\odot}$ .

Although our survey shows that the total CO luminosity of M31 is  $\sim 4$  times less than that of the Milky Way, and the peak CO surface brightness is  $\sim 6$  times less, it is less certain that the molecular mass is lower by a comparable factor. However, for several reasons we think it is likely to be lower by at least a factor of 2. First, CO observations of the LMC (Cohen et al. 1988) and SMC (Rubio et al. 1991) suggest that  $X$  may increase with decreasing metallicity, but the metallicity of M31 does not appear to differ significantly from that of the Milky Way (Blair, Kirshner, & Chevalier 1982; Dennefeld & Kunth 1981). Second, high-resolution CO observations of M31 (Boulanger

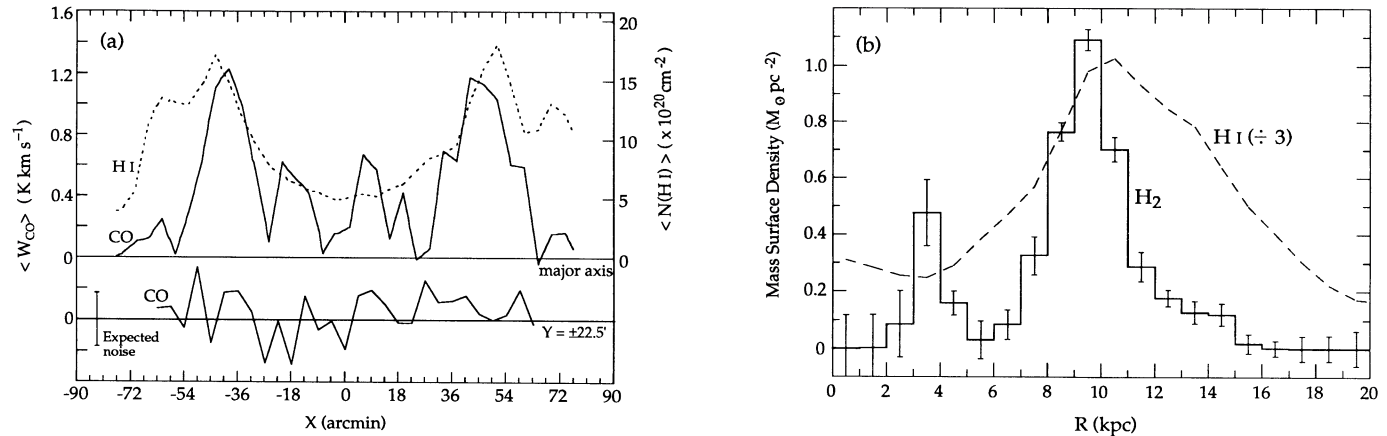


FIG. 3.—(a) Profile of  $W_{\text{CO}}$  averaged over a  $9'$  strip centered on the major axis compared with H I column density averaged over the same region. For  $X > 0$ , the major axis was assumed to follow p.a.  $38^\circ$  (as in Fig. 1 and elsewhere in the paper), but to account for an apparent offset of the SW tangent region, for  $X < 0$  it was assumed to be at p.a.  $33^\circ$ , to pass through the CO and H I peaks at  $(-45', 4.5')$ . Below is a similar profile from above and below the molecular disk ( $Y = \pm 22.5'$ ), to demonstrate the absence of systematic errors. (b) Radial distributions of atomic and molecular mass surface densities in M31, from a fit of axisymmetric models to the  $N_{\text{H I}}$  and  $W_{\text{CO}}$  maps in Fig. 2. Molecular column densities were calculated using  $N(\text{H}_2)/W_{\text{CO}} = 2.3 \times 10^{20} \text{ cm}^{-2} \text{ K}^{-1} \text{ km}^{-1} \text{ s}$  (Strong et al. 1988) and on the assumption of a distance of 690 kpc and an inclination of  $77^\circ$  for M31. The error bars represent  $1 \sigma$  instrumental noise.

et al. 1984, 1988; Casoli, Combes, & Stark 1987; Lada et al. 1988; Vogel, Boulanger, & Ball 1987) show that the large molecular clouds there are apparently similar to those in the Milky Way. And third—and perhaps most important—the average rate of star formation in M31 relative to that in the Milky Way seems to be lower in rough proportion to its lower molecular gas content. Specifically, the integrated luminosity of M31 in the infrared is  $\sim 6$  times less than that of the Milky Way, and in nonthermal continuum radiation (408 MHz)  $\sim 12$  times less (Walterbos 1986, and references therein), and the disk of M31 has a volume emissivity at 2695 MHz  $\sim 6$  times lower (Berkhuijsen 1977).

Why M31 and the Milky Way, two spiral galaxies with comparable amounts of atomic gas, differ in molecular content by a factor of 4 remains an open and interesting question. Beyond 8 kpc the radial distributions of H I and H<sub>2</sub> in these

galaxies are quite similar, both falling off exponentially from values of  $\sim 3 M_{\odot} \text{ pc}^{-2}$  and  $\sim 1 M_{\odot} \text{ pc}^{-2}$ , respectively, at that radius. The two galaxies are also similar in having large central holes deficient in both atomic and molecular gas, although M31 seems to lack entirely the dense nuclear region in the center of this hole so prominent in our galaxy. An essential difference seems to be the sizes of the central holes: about 3 kpc in radius for the Milky Way compared with about 7 kpc for M31. In the Milky Way the molecular surface density continues to increase inward from  $R_{\odot}$  to a peak near 4.5 kpc, but in M31 a similar increase is prohibited by the sharp decline in total gas density. A possible cause for the larger central hole in M31 may be the very prominent bulge ( $L_{\text{blue}} = 6.4 \times 10^9 L_{\odot}$ ; Walterbos & Kennicutt 1988), more than 4 times as luminous in visible light as the bulge of the Milky Way ( $1.5 \times 10^9 L_{\odot}$ ; van der Kruit 1986).

#### REFERENCES

- Arp, H. 1964, *ApJ*, 139, 1045  
 Berkhuijsen, E. M. 1977, *A&A*, 57, 9  
 Berkhuijsen, E. M., Beck, R., & Gräve, R. 1987, in *Interstellar Magnetic Fields*, ed. R. Beck & R. Gräve (Berlin: Springer), 38  
 Berkhuijsen, E. M., Wielebinski, R., & Beck, R. 1983, *A&A*, 117, 141  
 Blair, W. P., Kirshner, R. P., & Chevalier, R. A. 1982, *ApJ*, 254, 50  
 Boulanger, F., Bystedt, J., Casoli, F., & Combes, F. 1984, *A&A*, 140, L5  
 Boulanger, F., Stark, A. A., & Combes, F. 1981, *A&A*, 93, L1  
 Boulanger, F., Vogel, S. N., Viallefond, F., & Ball, R. 1988, in *Molecular Clouds in the Galaxy and External Galaxies*, ed. R. L. Dickman, R. L. Snell, & J. S. Young (Berlin: Springer), 401  
 Bronfman, L., Cohen, R. S., Alvarez, H., May, J., & Thaddeus, P. 1988, *ApJ*, 324, 248  
 Casoli, F., Combes, F., & Stark, A. A. 1987, *A&A*, 173, 43  
 Cohen, R. S., Dame, T. M., Garay, G., Montani, J., Rubio, M., & Thaddeus, P. 1988, *ApJ*, 331, L95  
 Combes, F., Encenaz, P. J., Lucas, R., & Weliachew, L. 1977, *A&A*, 61, L7  
 Cram, T. R., Roberts, M. S., & Whitehurst, R. N. 1980, *A&AS*, 40, 215  
 Dennefeld, M., & Kunth, D. 1981, *ApJ*, 86, 989  
 Digel, S. W. 1991, Ph.D. thesis, Harvard Univ.  
 D'Odorico, S., Dopita, M. A., & Benvenuti, P. 1980, *A&AS*, 40, 67  
 Habing, H. J., et al. 1984, *ApJ*, 278, L59  
 Hodge, P. W. 1980, *AJ*, 85, 376  
 Ichikawa, T., Nakano, M., Tanaka, Y. D., & Saito, M. 1985, *PASJ*, 37, 439  
 Lada, C. J., Margulis, M., Sofue, Y., Nakai, N., & Handa, T. 1988, *ApJ*, 328, 143  
 Lucy, L. B. 1974, *AJ*, 79, 745  
 Pellet, A., Astier, N., Viale, A., Courté, G., Maucherat, A., Monnet, G., & Simien, F. 1978, *A&AS*, 31, 439  
 Rubio, M., Garay, G., Montani, J., & Thaddeus, P. 1991, *ApJ*, 368, 173  
 Ryden, B. S., & Stark, A. A. 1986, *ApJ*, 305, 823  
 Stark, A. A. 1985, in *The Milky Way Galaxy*, ed. H. van Woerden, R. J. Allen, & W. B. Burton (Dordrecht: Reidel), 445  
 Stark, A. A., Linke, R. A., & Frerking, M. A. 1981, *BAAS*, 13, 535  
 Strong, A. W., et al. 1988, *A&A*, 207, 1  
 Unwin, S. C. 1980, *MNRAS*, 192, 243  
 van der Kruit, P. C. 1986, *A&A*, 157, 230  
 Vogel, S. N., Boulanger, F., & Ball, R. 1987, *ApJ*, 321, L145  
 Walterbos, R. A. M. 1986, Ph.D. thesis, Leiden Univ.  
 Walterbos, R. A. M., & Kennicutt, R. C. 1988, *A&A*, 198, 61  
 Walterbos, R. A. M., & Schwing, P. B. W. 1987, *A&A*, 180, 27  
 Young, J. S., & Scoville, N. Z. 1991, *ARA&A*, 29, 581